

# Linear-optical frequency beamsplitter for fiber-optic quantum networks

Hsuan-Hao Lu,<sup>1</sup> Joseph M. Lukens,<sup>2</sup> Nicholas A. Peters,<sup>2,3</sup> Ogaga D. Odele,<sup>1</sup> Andrew M. Weiner,<sup>1</sup> and Pavel Lougovski<sup>2,\*</sup>

<sup>1</sup>*School of Electrical and Computer Engineering and Purdue Quantum Center,  
Purdue University, West Lafayette, Indiana 47907, USA*

<sup>2</sup>*Quantum Information Science Group, Oak Ridge National Laboratory, Oak Ridge, Tennessee 37831, USA*

<sup>3</sup>*Bredesen Center for Interdisciplinary Research and Graduate Education,  
The University of Tennessee, Knoxville, Tennessee 37996, USA*

(Dated: April 26, 2017)

We experimentally implement a frequency beamsplitter for spectrally encoded photons, based on electro-optic modulation and Fourier-transform pulse shaping. The beamsplitter offers near-unity fidelity (up to  $0.99998 \pm 0.00003$ ), maintains high performance across the entire C-band (1530–1570 nm), and can operate concurrently on two qubits spaced as tightly as four modes apart. The new gate represents an important building block toward scalable and robust quantum networks based on frequency-multiplexed quantum interconnects.

## I. INTRODUCTION

A key component on the path to the “quantum internet” [1, 2]—the vision for a universal network for quantum computation, communication, and cryptography—is the *quantum interconnect*, which relies on entanglement swapping to entangle distant qubits that cannot otherwise couple to each other. Two archetypal examples are the DLCZ [3] and Duan-Kimble [4] protocols. In both approaches, two spatially separated atomic systems are entangled with photonic modes locally; the two optical modes are transmitted to a common location where, depending on the protocol, either a single- or two-photon interference experiment is performed; upon photon detection, the atomic qubits are projected onto the desired entangled state. Multiple interconnect variations have grown out of these original protocols, but all contain these essential two steps: (1) entangle matter qubits with photons locally, and (2) mix and detect the photons to entangle the isolated matter qubits with each other. Depending on the scheme, photon mixing can be realized with spatial or polarizing beamsplitters.

The interconnect above requires complete indistinguishability of the photons from each qubit. In particular, the wavelengths of all photonic modes must be identical to within their overall bandwidth, a prerequisite difficult to satisfy for heterogeneous qubit systems with distinct transition frequencies, or even for matched qubit species surrounded by different local environments. Yet rather than viewing this frequency mismatch as a nuisance requiring correction, we can actually exploit it for entanglement swapping directly. Indeed, as detailed by some of us in a recent proposal [5], universal quantum computing is attainable in a fiber-optic system comprising only photonic frequency qubits, Fourier-transform pulse shapers, and electro-optic phase modulators (EOMs). Moreover, the quantum interconnect protocols in [3, 4] can be easily recast to operate on the photonic spectral degree of freedom. In this work, we experimentally demonstrate a fundamental component of these schemes: the frequency beamsplitter, or Hadamard gate. Our spectral beamsplitter attains

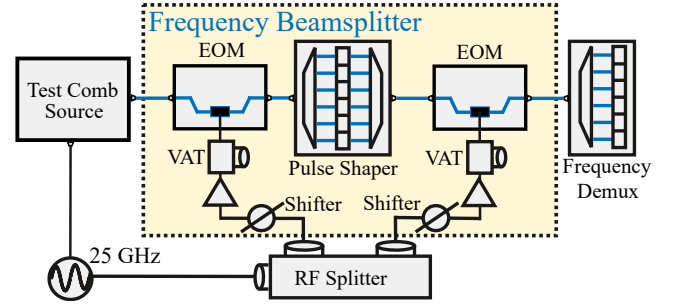


FIG. 1. Experimental setup. The spectral beamsplitter consists of two EOMs driven by phase-shifted 25-GHz sinewaves, with a pulse shaper in between. To characterize performance, an electro-optic frequency comb source inputs a coherent state in an arbitrary spectral superposition, and the power in each frequency mode is measured at the output, either with an optical spectrum analyzer or single-photon detector.

near-unity fidelity, preserves high performance across the entire optical C-band around 1550 nm, and can operate in parallel on multiple two-mode sets (qubits) spaced only a few frequency modes apart. Our results suggest broad applicability to frequency-based quantum interconnects, as well as to spectral quantum information processing more generally. With our spectral beamsplitter, energy-mismatched matter qubits can now be interconnected directly, without the need for an additional quantum frequency conversion step.

## II. THEORY

The photonic Hilbert space under consideration consists of a single spatio-polarization mode containing a comb of narrowband modes with frequencies  $\omega_n = \omega_0 + n\Delta\omega; n \in \mathbb{Z}$ . Logical zero corresponds to a photon at frequency  $\omega_0$ :  $|0\rangle_L = |1_{\omega_0} 0_{\omega_1}\rangle = \hat{a}_{\omega_0}^\dagger |\text{vac}\rangle$ . Logical 1 signifies a photon at frequency  $\omega_1$ :  $|1\rangle_L = |0_{\omega_0} 1_{\omega_1}\rangle = \hat{a}_{\omega_1}^\dagger |\text{vac}\rangle$ . Now suppose that frequencies  $\omega_0$  and  $\omega_1$  correspond to the resonances of atomic spin systems *A* and *B*, respectively, such that the single-photon portion of the joint matter-field state, following optical excitation,

\* lougovskip@ornl.gov

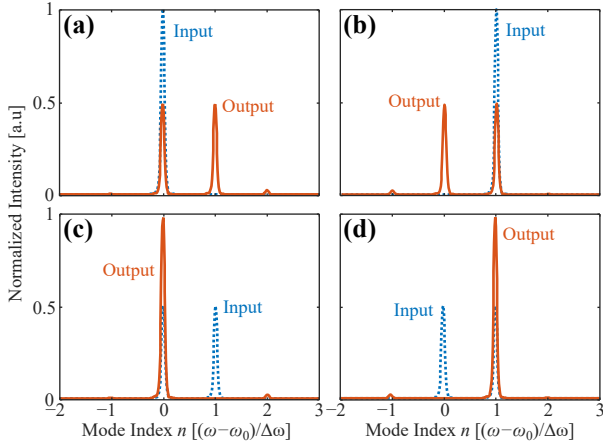


FIG. 2. Experimentally measured beamsplitter output spectra for specific coherent state inputs. (a) Pure mode 0:  $|\alpha_{\omega_0} 0_{\omega_1}\rangle$ . (b) Pure mode 1:  $|0_{\omega_0} \alpha_{\omega_1}\rangle$ . (c) Mode 0 and mode 1 in phase:  $|\alpha_{\omega_0} \alpha_{\omega_1}\rangle$ . (d) Mode 0 and mode 1 out of phase:  $|\alpha_{\omega_0} (-\alpha)_{\omega_1}\rangle$ .

looks like

$$|\psi\rangle \sim |\uparrow\downarrow\rangle_{AB}|1_{\omega_0} 0_{\omega_1}\rangle + |\downarrow\uparrow\rangle_{AB}|0_{\omega_0} 1_{\omega_1}\rangle. \quad (1)$$

In the context of a DLCZ-like quantum interconnect [3] for this situation, a 50:50 frequency beamsplitter implements the Hadamard operation

$$H = \frac{1}{\sqrt{2}} \begin{pmatrix} 1 & 1 \\ 1 & -1 \end{pmatrix} \quad (2)$$

on the  $\omega_0, \omega_1$  space, leaving the state

$$|\tilde{\psi}\rangle \sim \left( |\uparrow\downarrow\rangle_{AB} + |\downarrow\uparrow\rangle_{AB} \right) |1_{\omega_0} 0_{\omega_1}\rangle + \left( |\uparrow\downarrow\rangle_{AB} - |\downarrow\uparrow\rangle_{AB} \right) |0_{\omega_0} 1_{\omega_1}\rangle. \quad (3)$$

Frequency-resolved photon detection then projects onto a maximally entangled atomic state.

On the other hand, a polarizing beamsplitter—a key component of a Duan-Kimble interconnect [4]—in spectral encoding can be viewed as a four-mode frequency transformation  $U$  on modes labeled  $\omega_0, \dots, \omega_3$ . It is easy to show that  $U$  is decomposable as

$$U = \begin{pmatrix} H & 0 \\ 0 & H \end{pmatrix} \begin{pmatrix} \mathbb{1} & 0 \\ 0 & P \end{pmatrix} \begin{pmatrix} H & 0 \\ 0 & H \end{pmatrix}, \quad (4)$$

where  $P = \text{diag}(1, -1)$  and  $\mathbb{1}$  is the  $2 \times 2$  identity matrix. Thus, realizing the Hadamard mode transformations in parallel enables Duan-Kimble-like entanglement swapping as well.

If the implemented network can be represented as a linear transformation on the mode operators, i.e.,  $\hat{a}_{\omega_n, \text{out}} = \sum_k W_{nk} \hat{a}_{\omega_k, \text{in}}$ , then we can quantify performance against the ideal operation  $H$  via the fidelity

$$\mathcal{F} = \frac{\text{Tr}(W^\dagger H) \text{Tr}(H^\dagger W)}{\text{Tr}(W^\dagger W) \text{Tr}(H^\dagger H)} \quad (5)$$

and success probability

$$\mathcal{P} = \frac{\text{Tr}(W^\dagger W)}{\text{Tr}(H^\dagger H)}. \quad (6)$$

An optimal gate realizes  $\mathcal{F} \rightarrow 1$  and  $\mathcal{P}$  as large as possible [6]. Experimentally, the probability of success is further degraded by photon loss, an effect absent in an ideal unitary network. But since linear insertion loss is distinct from operation purity (and in principle can be reduced with further system engineering), for experimental comparison below we normalize the measured linear transformation by total transmissivity before computing  $\mathcal{P}$ . Thus, a value  $\mathcal{P} = 1$  does not signify zero loss, but rather means that, given that the input photon exits the network, it is guaranteed to have undergone the desired operation and has not been scattered into adjacent modes.

In our previous theoretical work [5], this operation was found attainable with a series of alternating EOMs and pulse shapers. Incidentally, we note that alternative frequency beamsplitters based on nonlinear optical processes have been demonstrated as well, both in  $\chi^{(2)}$  [7] and  $\chi^{(3)}$  [8] systems. Nonlinear approaches have the advantage of supporting much wider frequency separations, but the disadvantages of requiring strong pump fields and careful phase matching which, in the  $\chi^{(3)}$  case, necessitate low temperatures to suppress Raman noise [8]. Moreover, by energy conservation, any attempt at parallelization requires additional pump wavelengths to enable multiple frequency pairs to mix. On the other hand, because our version is optically linear, in that performance is independent of optical power, high-visibility interference is obtained naturally and at room temperature, with detector dark counts providing the only measurable noise. And as shown below, the electro-optic interaction is largely immune to translation of the absolute wavelength, making parallelization simple and direct. Therefore, our electro-optic approach excels for tightly spaced modes operated on in parallel—as in, e.g., a dense wavelength-division multiplexed system—whereas a nonlinearity-based beamsplitter would make the most sense for interband modes spaced beyond typical electro-optic bandwidths.

### III. EXPERIMENT

Figure 1 provides a schematic of the experimental setup. The frequency mode spacing is  $\Delta\omega = 2\pi \times 25$  GHz. Simplifying our original proposal slightly, we found in further simulations that three total components (EOM-shaper-EOM) suffice to perform the Hadamard gate, rather than four. And instead of driving each EOM with an arbitrary waveform for theoretically perfect performance, we also found that using only phase-shifted sinewaves attains fidelity  $\mathcal{F} = 0.9999$  and success probability  $\mathcal{P} = 0.9760$ , only a small reduction. Therefore, for this proof-of-principle demonstration, we utilize a single 25-GHz tone for modulation, with the understanding that 100% fidelity and success probability can be achieved with more complicated drive waveforms.

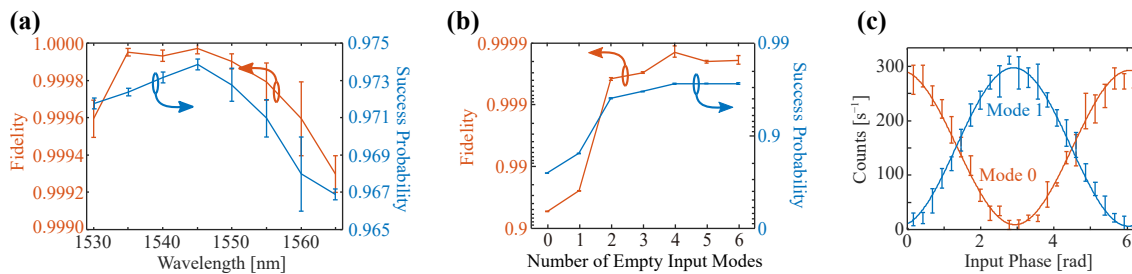


FIG. 3. (a) Fidelity and success probability as a function of center wavelength. (b) Parallel beamsplitter performance against frequency separation. (c) Output counts for frequency superposition single-photon input, as the relative phase is scanned.

First, to characterize the frequency mode transformation, we probe the network with a classical electro-optic frequency comb, measuring the output spectrum for different frequency superpositions. This technique represents the spectral analogue of the spatial version presented in [9] and greatly simplifies initial characterization. Conceptually, one can understand the legitimacy of this procedure because the operation of interest is, at its basic level, a linear network; thus its distinguishing behavior holds for high-flux coherent states as well as single photons. Operating at a center wavelength of 1545.04 nm ( $\omega_0 = 2\pi \times 194.036$  THz), we measure fidelity  $\mathcal{F} = 0.99998 \pm 0.00003$  and success probability  $\mathcal{P} = 0.9739 \pm 0.0003$ , normalized by insertion loss. Figure 2 shows four examples of experimentally recorded input/output combinations: the top row shows the equi-amplitude superpositions resulting from input in either mode 0 or mode 1; the second row reveals the single-wavelength output with the input in the states  $|\alpha_{\omega_0}(\pm\alpha)_{\omega_1}\rangle$ . The small bumps in adjacent modes  $-1$  and  $+2$  reflect the nonunity success probability, a limitation which—as noted above—could be removed by more sophisticated modulation waveforms.

A crucial claim in favor of our beamsplitter is its suitability for parallelization. To examine this aspect in detail, we scan the wavelength of the central gate mode in 5-nm increments and measure  $\mathcal{F}$  and  $\mathcal{P}$  at each step. Figure 3(a) shows that the fidelity exceeds 99.9% for all test points, and the success probability does not drop below 96.5%. A second question, complementary to the total acceptance bandwidth, is the minimum frequency spacing: how close can the frequencies of two gates be placed without performance degradation? Since sidebands adjacent to the computational space are populated mid-calculation, one would expect that a finite

number of dark, buffer modes are required to prevent cross-contamination. We address this question experimentally by implementing two beamsplitters in parallel and characterizing the total operation as a function of the number of initially empty modes between mode 1 of the low-frequency gate and mode 0 of the higher frequency one. The fidelity and success probability of the parallel operation are plotted in Fig. 3(b); they reach their limiting values for separations of just four modes. Combined with the 40-nm (5-THz) bandwidth of Fig. 3(a) and the mode spacing of 25 GHz, these findings imply that approximately 33 frequency beamsplitters could be implemented in parallel in this device—a remarkable indication of the promise of our approach in scalable quantum networks.

Finally, we attenuate the input to  $\sim 0.1$  photons per detection window and scan the phase  $\phi$  of the state  $|\psi\rangle = |1_{\omega_0}0_{\omega_1}\rangle + e^{i\phi}|0_{\omega_0}1_{\omega_1}\rangle$  in the single-photon subspace. At each setting, we use a wavelength-selective switch to direct the output modes to an InGaAs single-photon detector. Figure 3(c) plots the counts in modes  $\omega_0$  and  $\omega_1$  after subtracting the average dark count rate, showing the expected sinusoidal oscillations. The visibilities are  $\sim 92$ – $93\%$ ; at higher photon fluxes, values in excess of 98% were observed, confirming that the primary limitation is dark count fluctuations, rather than the operation itself. These results indicate excellent beamsplitter performance at the single-photon level as well, highlighting its applicability to quantum interconnects.

**Acknowledgments.** This work was performed in part at Oak Ridge National Laboratory, operated by UT-Battelle for the U.S. Department of Energy under contract no. DE-AC05-00OR22725. Funding was provided by ORNL’s Laboratory Directed Research and Development Program and National Science Foundation grant ECCS-1407620.

[1] H. J. Kimble, *Nature* **453**, 1023 (2008).  
 [2] S. Pirandola and S. L. Braunstein, *Nature* **532**, 169 (2016).  
 [3] L.-M. Duan, M. D. Lukin, J. I. Cirac, and P. Zoller, *Nature* **414**, 413 (2001).  
 [4] L.-M. Duan and H. J. Kimble, *Phys. Rev. Lett.* **90**, 253601 (2003).  
 [5] J. M. Lukens and P. Lougovski, *Optica* **4**, 8 (2017).  
 [6] D. B. Uskov, L. Kaplan, A. M. Smith, S. D. Huver, and J. P. Dowling, *Phys. Rev. A* **79**, 042326 (2009).

[7] T. Kobayashi, R. Ikuta, S. Yasui, S. Miki, T. Yamashita, H. Terai, T. Yamamoto, M. Koashi, and N. Imoto, *Nat. Photon.* **10**, 441 (2016).  
 [8] S. Clemmen, A. Farsi, S. Ramelow, and A. L. Gaeta, *Phys. Rev. Lett.* **117**, 223601 (2016).  
 [9] S. Rahimi-Keshari, M. A. Broome, R. Fickler, A. Fedrizzi, T. C. Ralph, and A. G. White, *Opt. Express* **21**, 13450 (2013).